

# Monitoring the dye impregnation time of nanostructured photoanodes for dye sensitized solar cells

**N. Shahzad**<sup>a,b</sup>, D. Pugliese<sup>a,b</sup>, A. Lamberti<sup>a,b</sup>, A. Sacco<sup>a,b</sup>, A. Virga<sup>b</sup>, R. Gazia<sup>a</sup>, S. Bianco<sup>a,b</sup>, M. I. Shahzad<sup>b</sup>, E. Tresso<sup>a,b</sup> and C. F. Pirri<sup>a,b</sup>

<sup>a</sup> Center for Space Human Robotics @PoliTo, Istituto Italiano di Tecnologia, Corso Trento 21, Torino, IT-10129, Italy

<sup>b</sup> Applied Science and Technology Department (DISAT), Politecnico di Torino, Corso Duca degli Abruzzi 24, Torino, IT-10129, Italy

**Corresponding Author:**

**Nadia Shahzad**

DISAT, Politecnico di Torino,  
Corso Duca Degli Abruzzi-24, Torino-10128, Italy  
Tel: +39 011 090 7380-48, Fax: +39 011 090 7399  
Email: [nadia.shahzad@polito.it](mailto:nadia.shahzad@polito.it)

**Abstract.** Dye-sensitized solar cells (DSSCs) are getting increasing attention as low-cost, easy-to-prepare and colored photovoltaic devices. In the current work, in view of optimizing the fabrication procedures and understanding the mechanisms of dye attachment to the semiconductor photoanode, absorbance measurements have been performed at different dye impregnation times ranging from few minutes to 24 hours using UV-Vis spectroscopy. In addition to the traditional absorbance experiments, based on diffuse and specular reflectance on dye impregnated thin films and on the desorption of dye molecules from the photoanodes by means of a basic solution, an alternative in-situ solution depletion measurement, which enables fast and continuous evaluation of dye uptake, is presented. Photoanodes have been prepared with two different nanostructured semiconducting films: mesoporous TiO<sub>2</sub>, using a commercially available paste from *Solaronix*, and sponge-like ZnO obtained in our laboratory from sputtering and thermal annealing. Two different dyes have been analyzed: Ruthenizer 535-bisTBA (N719), which is widely used because it gives optimal photovoltaic performances, and a new metal-free organic dye based on a hemisquaraine molecule (CT1). Dye sensitized cells were fabricated using a customized microfluidic architecture. The results of absorbance measurements are presented and discussed in relation to the obtained solar energy conversion efficiencies and the incident photon-to-electron conversion efficiencies (IPCE).

## 1. Introduction

Dye-Sensitized Solar Cells (DSSCs) have attracted widespread interest since their first description by Grätzel and O'Regan [1] as an influential and low cost solar energy harvester. In a conventional DSSC, the photoanode consists of a TiO<sub>2</sub> layer (8-15 μm) deposited on a Transparent Conducting Oxide (TCO) covered glass substrate and sensitized with dye molecules (usually Ru complexes). An electrolyte containing I<sup>-</sup>/I<sub>3</sub><sup>-</sup> redox couple acts as hole conductor and electrically regenerate the dye molecules. Another TCO covered substrate with a thin Pt layer (few nm) serves as counter electrode, to promote the reduction of the triiodide [2, 3]. In these cells, the sensitizer plays an important role: it is responsible for the electric current generation, by harvesting the solar radiation and injecting the excited electrons into the semiconductor conduction band. Consequently, the dying process has an elemental impact on both cell performance and scale-up viewpoint. Existing dye uptake



measurements are based on dye desorption from photoanode after specified time intervals using a basic (*e.g.* NaOH or KOH) solution, and the subsequent UV-Vis spectroscopy. Although this procedure is quantitative, it is destructive of the devices and most of all *in-situ* measurements are impracticable. In alternative, the so-called solution depletion method is a powerful way to monitor dying processes [4, 5].

Over the last 20 years, ruthenium complexes gifted with thiocyanate ligands have achieved power conversion efficiencies beyond 11% and showed good stability [6-8]. Nevertheless, metal-free organic dyes have attracted considerable attention for practical applications because of the high cost and rarity of Ru metal. In comparison to the ruthenium sensitizers, the obtained lower efficiencies of organic dyes are mainly due to the formation of dye aggregates on the semiconductor surface and to their narrow dye absorption bands in the visible region. Therefore, lots of efforts have been made to study organic dye molecules with broader spectral responses and higher molar extinction coefficients. [9-11].

Another key component, which is responsible of the dye absorption in the DSSCs is the nanostructured semiconductor oxide. The highest photovoltaic conversion efficiencies have been obtained for TiO<sub>2</sub>-photoanodes impregnated not only with Ru-based dyes but also organic sensitizers [6-11]. ZnO photoanodes, having the interesting property of higher specific surface area available for dye loading, have also been suggested. Many research groups have tried to investigate different ZnO nanostructures, such as nanowires, nanorods, platelets and branched structures, which exhibit great surface-to-volume ratio [12]. Moreover ZnO has attractive electronic properties [13] and nowadays the conversion efficiencies of ZnO based DSSCs, employing the Ru-based N719 dye, have been improved exceeding 6% [14, 15].

Aim of this work is to monitor the dye absorption in view of understanding the mechanisms of dye attachment to the semiconductor photoanode and of optimizing the assembly procedures in DSSCs. We have chosen to investigate two different semiconductor oxides: the traditionally employed nanostructured TiO<sub>2</sub> and a sponge-like ZnO film fabricated by sputtering in our laboratory. We have decided to compare the dye absorption properties of two different dyes: the largely used Ru-based N719 and a recently proposed organic dye [16] based on the hemisquaraine molecule (CT1).

## 2. Experimental details

### 2.1. Preparation of Electrodes

Fluorine-doped tin oxide (FTO) covered glasses (7 Ω/sq, Solaronix) were firstly cleaned by immersing in acetone in an ultrasonic bath for 10 minutes and rinsing with isopropanol. Afterwards the glasses were dipped for other 10 minutes in a 1:3 (Hydrogen Peroxide: Sulphuric Acid) piranha solution, so as to remove organic residues, rinsed with deionised water and finally dried using Nitrogen-shower. Then, a TiO<sub>2</sub> layer (Ti-Nanoxide D37, Solaronix) with a circular shape (nearly 1cm in diameter) was deposited onto FTO covered glasses by doctor blading technique described elsewhere [2]. The deposited films were then dried at 50 °C for 10 minutes on a hot plate and left for half an hour at ambient temperature. A subsequent sintering process at 450 °C for 30 minutes enabled the formation of nanoporous TiO<sub>2</sub> film with a mean thickness of 8.5 μm, as measured by a profilometer (P.10 KLA-Tencor Profiler). Post-treatment with TiCl<sub>4</sub> was performed according to the method described in literature [17, 18]. Briefly, an aqueous stock solution of 2 M TiCl<sub>4</sub> was diluted to 0.05 M. Freshly sintered TiO<sub>2</sub> films were immersed into this solution and placed on a hot plate at 70°C for 30 min in a closed hood. After TiCl<sub>4</sub> treatment, the films were again sintered at 450°C for 30 minutes.

Zn nanostructured layers (5 μm) were deposited on glasses coated with FTO by RF magnetron sputtering technique. The geometry of the sputtered layer was defined by covering the substrate with a hard circular mask. In order to obtain sponge-like ZnO layers, the deposited films were placed on a hot plate at 380 °C for 60 minutes in ambient air [19].

Photoanodes were immersed into a dye solution for different time periods at room temperature and then rinsed in ethanol to remove the unadsorbed dye molecules. For each impregnation time, eight anodes were prepared: five for cell fabrication and the remaining three for dye desorption procedure. Table 1 gives parameters for four different combinations of semiconducting oxide and dye.

**Table 1:** Photoanode parameters.

	Semiconducting Oxide	Dye	Solvent	Concentration of dye solution
Set 1	TiO <sub>2</sub>	N719 (Ruthenizer 535bis-TBA)	Ethanol	0.33mM
Set 2	TiO <sub>2</sub>	CT1 (Hemisquaraine)	Acetonitrile	0.17mM
Set 3	ZnO	N719 (Ruthenizer 535bis-TBA)	Ethanol	0.25mM
Set 4	ZnO	CT1 (Hemisquaraine)	Acetonitrile	0.17mM

For the fabrication of counter electrodes, two small pin-holes as inlet/outlet ports for electrolyte filling were drilled in the FTO glass substrate using powder blasting technology. Substrates were then cleaned with the same cleaning method described above and thermal evaporation was employed to deposit a 5 nm Pt thin film.

## 2.2. Cell Fabrication

Dye sensitized cells were fabricated employing a customized microfluidic architecture [20] consisting of a Poly-DiMethylSiloxane (PDMS) thin membrane reversibly sealed between the two electrodes with an external PolyMethylMethAcrylate (PMMA) clamping system. The structure of the cell is presented in figure 1. The electrolyte (Iodolyte AN 50, Solaronix) filling was performed with a syringe connected to the O-Ring PDMS interconnections. Copper foils (50  $\mu\text{m}$  thick, 1.5-cm<sup>2</sup> area) were used as electric contacts with FTO, dielectrically insulated by the PDMS membrane. Active area of the cells was 0.86 cm<sup>2</sup> and measurements were performed with a 0.22-cm<sup>2</sup> black rigid mask.

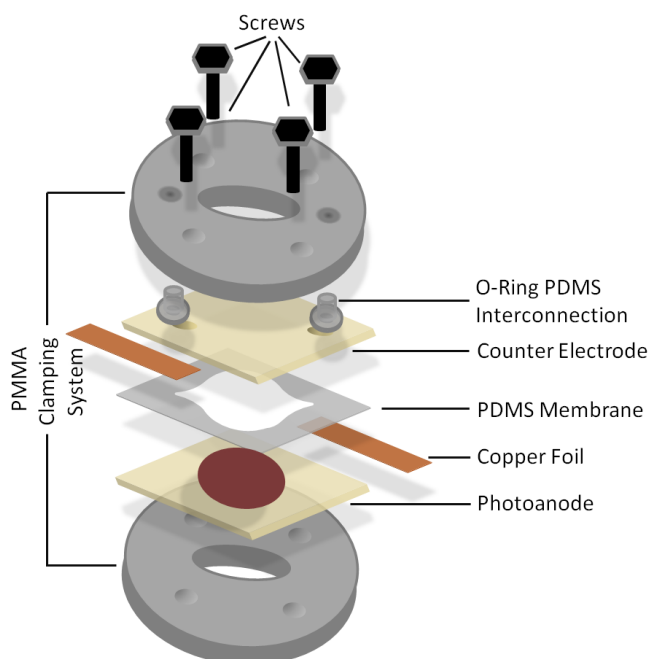


**Figure 1:** Scheme of the microfluidic dye-sensitized solar cell.

### 3. Characterizations

#### 3.1. Optical Measurements

**3.1.1. Photoanode Absorbance.** Photoanodes were optically characterized by UV-Vis spectrophotometer (Agilent, Varian Cary 5000) measuring Kubelka-Munk function,  $F(R)$ , utilizing integrating sphere as shown in figure 2a. The Kubelka-Munk theory is normally used for the analysis of diffuse reflectance spectra obtained from diffusing samples. It provides a correlation between reflectance and absorbance:  $F(R) = (1-R)^2/2R = k/s = A/c$  where  $R$  is the reflectance,  $k$  is the absorption coefficient,  $s$  is the scattering coefficient,  $A$  is the absorbance and  $c$  is the concentration of absorbing species. As  $c$  and  $s$  remain same, spectrum obtained for Kubelka-Munk function can be considered as absorbance.

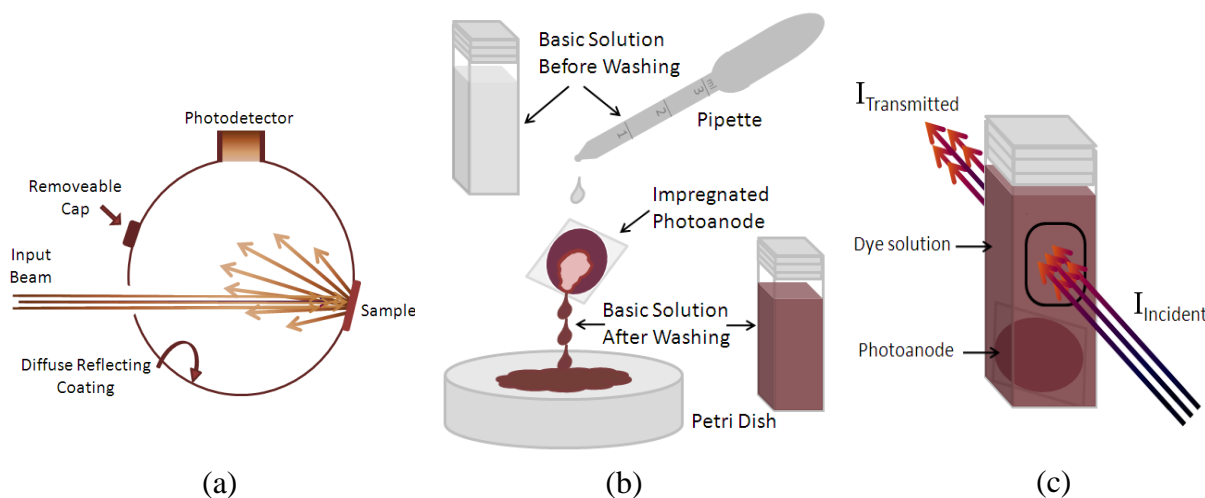


**Figure 2:** Schematic diagram of: (a) The integrating sphere for reflectance measurements, (b) washing procedure for dye loading measurements and (c) the solution depletion method to study the in situ uptake of dye molecules on the photoanode.

**3.1.2. Washing Procedure.** Investigation of dye loading amount was determined by desorbing the dye molecules from photoanode using a basic solution followed by measurement of the optical absorbance in optical density units with a UV-Vis spectrophotometer in the wavelength region from 300 to 800 nm. A simple but depictive scheme of the procedure is shown in figure 2b.

**3.1.3. Solution Depletion Method.** The sintered photoanode was immersed in a spectrophotometer quartz cuvette containing the dye solution consisting of 0.27mM N719 (Ruthenizer535bis-TBA, Solaronix) dye in ethanol (0.17mM hemisquaraine dye in acetonitrile). The cuvette with the immersed photoanode was placed in the UV-Vis spectrophotometer at room temperature for more than 24 hours in order to record the absorbance spectra. The photoanode was kept at the cuvette bottom as shown in the schematic diagram of the setup (figure 2c). This allowed monitoring of the depletion of dye solution with time, due to continuous adsorption of dye molecules by the photoanode. During the whole experiment cuvette was kept tightly covered with a cap to avoid the evaporation of solvent to make sure that the volume of solution remained constant. Experiment was repeated for three times to enhance the certainty of results.

#### 3.2. Electrical Measurements

I-V electrical characterizations were performed under AM1.5G illumination ( $1000 \text{ W/m}^2$ ) using a class A solar simulator (91195A, Newport) and a Keithley 2440 source measure unit. Incident photon-to-electron conversion efficiency (IPCE) measurements were carried out employing a 100-W QTH lamp (Newport) as light source and a 150-mm Czerny Turner monochromator (Omni-l 150, Lot-Oriel).

## 4. Results and Discussions

### 4.1. Nanostructured $\text{TiO}_2$ : absorption measurements

Figure 3 shows the absorption spectra of the dye-impregnated photoanodes of Set 1 (8.5  $\mu\text{m}$   $\text{TiO}_2$  films sensitized with N719) for different impregnation times, ranging from 3 to 24 hours. The spectra exhibit a typical trend, with the N719 absorption peaks located at 420 and 540 nm and superimposed to the  $\text{TiO}_2$  absorption (essentially located in the UV region). The dye-related peaks increase with the impregnation time as it was expected (except 24 hours). In order to have better evaluation of the dye absorption, the areas enclosed by the F(R) curves before and after dye incubation (which correspond respectively to the absorbance of the  $\text{TiO}_2$  and of the  $\text{TiO}_2$ /dye films) have been computed: these areas are a sort of “integrated” dye absorbance in the visible region. The results are shown in figure 3b, and they evidence that the increased light absorption of the photoanodes is due to an increased number of adsorbed dye molecules on the  $\text{TiO}_2$  film.

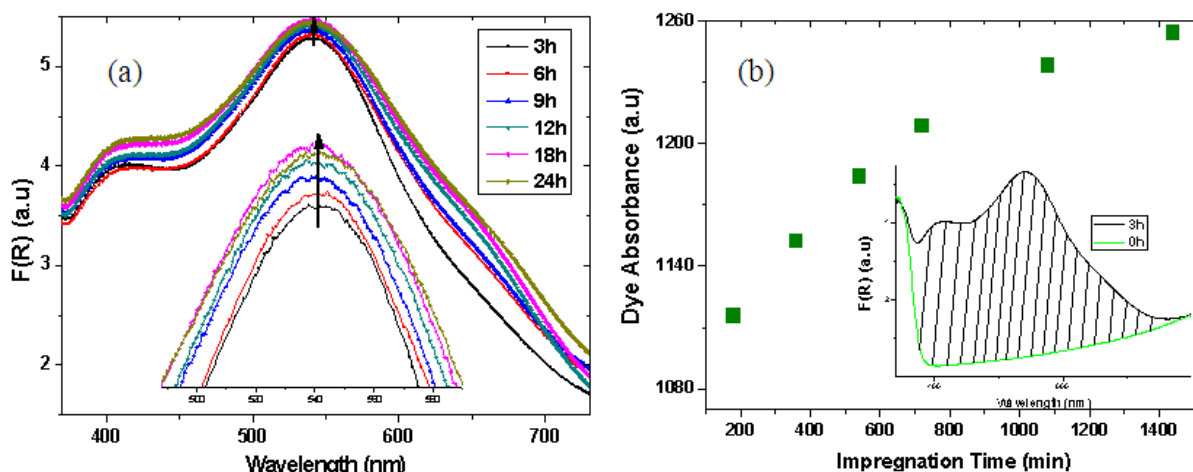


**Figure 3:** (a) Absorption spectra of photoanodes after dye impregnation for different time periods, (b) Area between F(R) curves after and before dye incubation (shown in inset only for 3h to have clear view).

For a quantitative analysis of dye loading, the washing procedure for desorption of dye from the anodes has been performed using a known volume of 0.1M NaOH aqueous solution, as implemented for different  $\text{TiO}_2$  nanostructures in literature [21-24]. The absorbance spectra of the resulting solutions are shown in the figure 4a. In addition, the depletion solution experiment has also been performed and the spectra are shown in figure 4b. When N719 is dissolved in a solvent it presents two narrow and well defined peaks, which are located at 386 and 530 nm when the solvent is ethanol, and at 372 and at 500 nm in aqueous solution of NaOH. By comparison with figure 3a it can be observed that the peaks are broadened and red-shifted when the dye is attached to the  $\text{TiO}_2$  film, this is due to the anchoring and to the chemical interaction of the dye molecules to the semiconductor surface.

From the spectra of figures 4a and 4b the concentration and hence the total number of adsorbed dye moles were calculated employing the Lambert-Beer law and the pre-determined extinction coefficient values:  $12717 \text{ M}^{-1} \text{ cm}^{-1}$  at 500 nm for the basic solution and  $14614 \text{ M}^{-1} \text{ cm}^{-1}$  at 529 nm for the ethanolic solution. The two dye incubation measures are compared in figure 4c and a strong correlation is observed in the obtained values of dye loading. The number of moles obtained from desorption is little lower than the one obtained from depletion. This dissimilarity can be due to an incomplete removal of dye molecules by the basic solution, or also to the fact that, after impregnation, the photoanodes are rinsed with ethanol. Such rinsing procedure removes also the physisorbed dye molecules which are not anchored to the  $\text{TiO}_2$  surface but are computed with the depletion method. In



any case, both the methods clearly show that there is an upper limit in the number of absorbed dye molecules and indicate that the saturation is reached at about 16 hours of impregnation time.

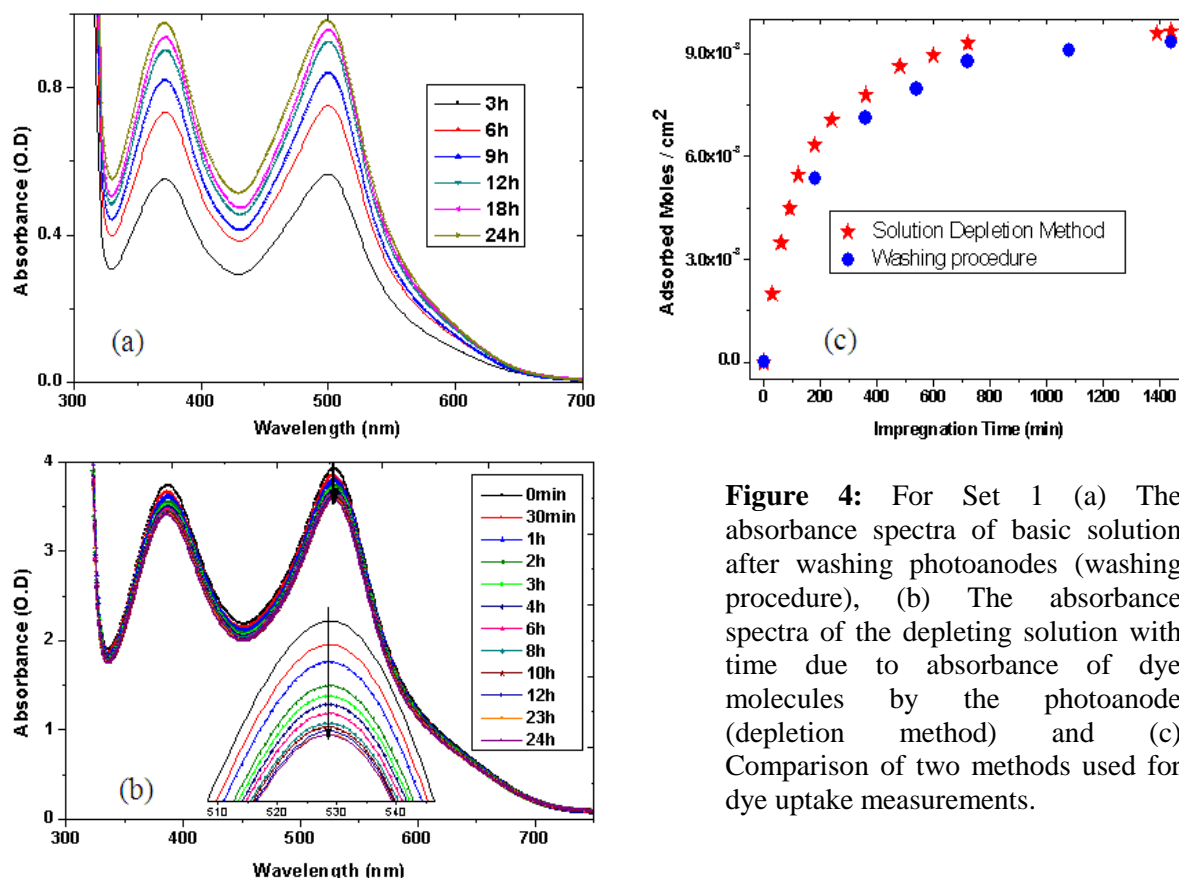


**Figure 4:** For Set 1 (a) The absorbance spectra of basic solution after washing photoanodes (washing procedure), (b) The absorbance spectra of the depleting solution with time due to absorbance of dye molecules by the photoanode (depletion method) and (c) Comparison of two methods used for dye uptake measurements.

The obtained results evidenced a well known behaviour of the N719 dye when attached to the  $\text{TiO}_2$  surface (in fact the typical impregnation time suggested for N719-based DSSCs is overnight [3, 21]), and they confirm that our experimental procedures for absorption evaluation are correct. We decided to apply these procedures to study the recently introduced hemisquaraine CT1 dye. This dye is prepared following a simple, easy and inexpensive three steps synthesis: quaternarization, coupling and hydrolysis, according to a classical procedure for hemisquaraine dyes [25]. The CT1 absorbance spectrum in acetonitrile solution is reported in figure 5a (Set 2). It exhibits a wide band composed by three neighboring peaks centered at 388nm, 419nm and 434nm with an average molar extinction coefficient of  $15220 \text{ M}^{-1}\text{cm}^{-1}$ . CT1 shows promising property of good light absorption, even if – compared to N719- the absorption extends only till 500 nm and does not cover the red region of the visible spectrum. The absorption spectra obtained on the CT1/ $\text{TiO}_2$  photoanodes are compared in the inset of figure 5b for impregnation times ranging from 2 min to 24 hours, where again a broadening and a red- shift of the peaks due to dye anchoring to the  $\text{TiO}_2$  surface is observed. Such a red-shift extends till 600 nm the CT1 region of light absorption. Moreover it can be observed that the peak at 480nm shows very small variation in intensity with increasing incubation period, while the 414 nm peak intensity strongly increases till 3 hours of impregnation, and remains nearly constant for longer times. Another shoulder-like peak appears only for impregnation times higher than 2-3 hours and it can be seen increasing up to 15 hours. The integrated dye absorbance of Set 2 (CT1 hemisquaraine dye/ $\text{TiO}_2$  photoanodes) shown in figure 5b has been obtained, as previously described, by calculating the area between the F(R) curves before and after dye impregnation.

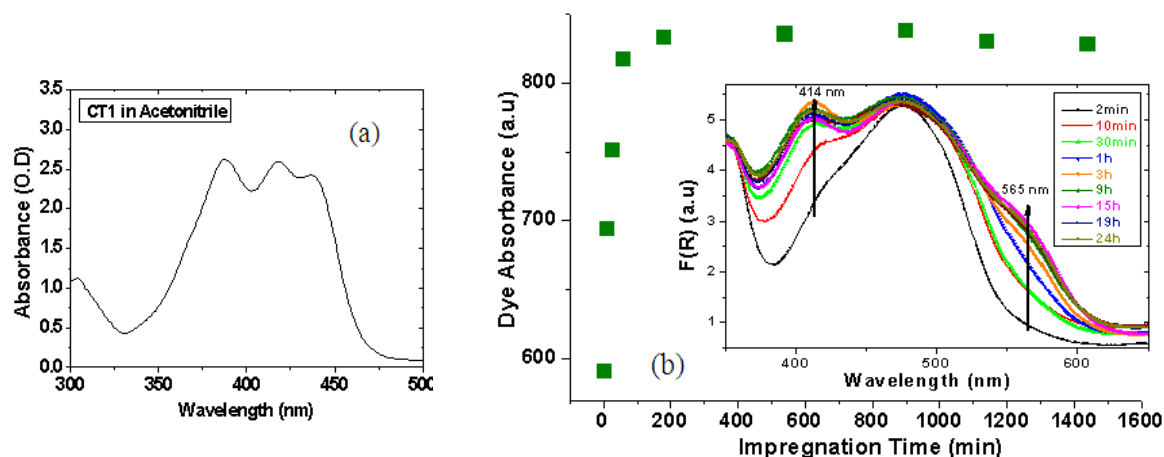


**Figure 5:** (a) Optical absorbance of hemi-squaraine dye in acetonitrile (b) Dye absorbance obtained by calculating area between the  $F(R)$  curves before and after dye impregnation. Inset compares the absorption spectrum of Set 2 (CT1 absorbed on  $\text{TiO}_2$  film).

For obtaining a quantitative analysis different tests have been performed for washing procedures of hemisquaraine dye from the  $\text{TiO}_2$  photoanodes: the best performing solution was found to be a 0.5M aqueous solution of KOH. Absorbance spectra of such basic solution after rinsing the photoanodes are shown in the figure 6a. The desorbed dye moles numbers were calculated using the extinction coefficient value ( $25715 \text{ M}^{-1} \text{ cm}^{-1}$  at 447 nm) of dye in the corresponding basic aqueous solution.

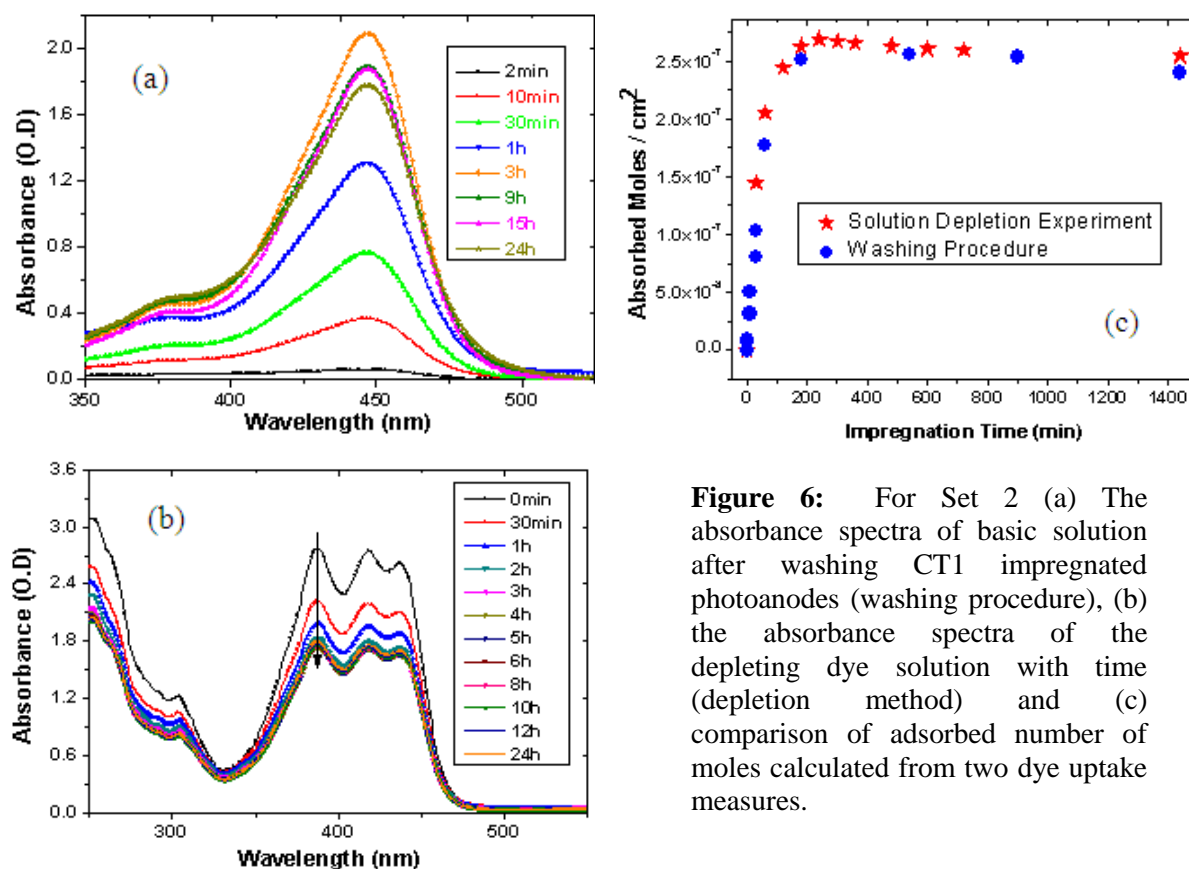


**Figure 6:** For Set 2 (a) The absorbance spectra of basic solution after washing CT1 impregnated photoanodes (washing procedure), (b) the absorbance spectra of the depleting dye solution with time (depletion method) and (c) comparison of adsorbed number of moles calculated from two dye uptake measures.

The absorbance spectra obtained from solution depletion experiment (shown in figure 6b) has been used to calculate the number of moles using molar extinction coefficient value of CT1 solution in acetonitrile which is  $15930 \text{ M}^{-1}\text{cm}^{-1}$  at 388 nm. Comparing the two measurements (figure 6c), it is found that the dye loading results are in agreement, with a little dissimilarity as it was also observed for the traditional dye N719. Both the methods reveal saturation at around 3 hours.

#### 4.2 - Nanostructured $\text{TiO}_2$ : Comparison with electrical measurements

The dye impregnated photoanodes of Set1 (N719/ $\text{TiO}_2$ ) and Set 2 (CT1/ $\text{TiO}_2$ ) have all been employed for fabrication of DSSCs. The dependence of the cell efficiency on dye incubation time was studied by I-V electrical characterization and incident photon-to-electron conversion efficiency (IPCE) measurements. The current density-voltage curves of Set 1 and Set 2 are reported in (a) and (b) parts of figure 7, respectively, as a function of incubation time. A monotonic behavior, with a saturating incubation time around 16 hours clearly appears for N719, while a non-monotonic trend, with favorable incubation time around 1 hour, is observed with CT1. Sections (c) and (d) of the same figure compare the IPCE curves of the N719 and hemisquaraine based DSSCs, respectively. For Set 2 (CT1 impregnated), the peak at about 460nm is blue shifted, lowered and broadened for impregnation times longer than 1h. This fact indicates degradation in the photon-to-current conversion, it can be related to the observed trend in the F(R) peak at 414 nm (figure 5a) and hence it can lead to a lower efficiency of the solar cell [26].

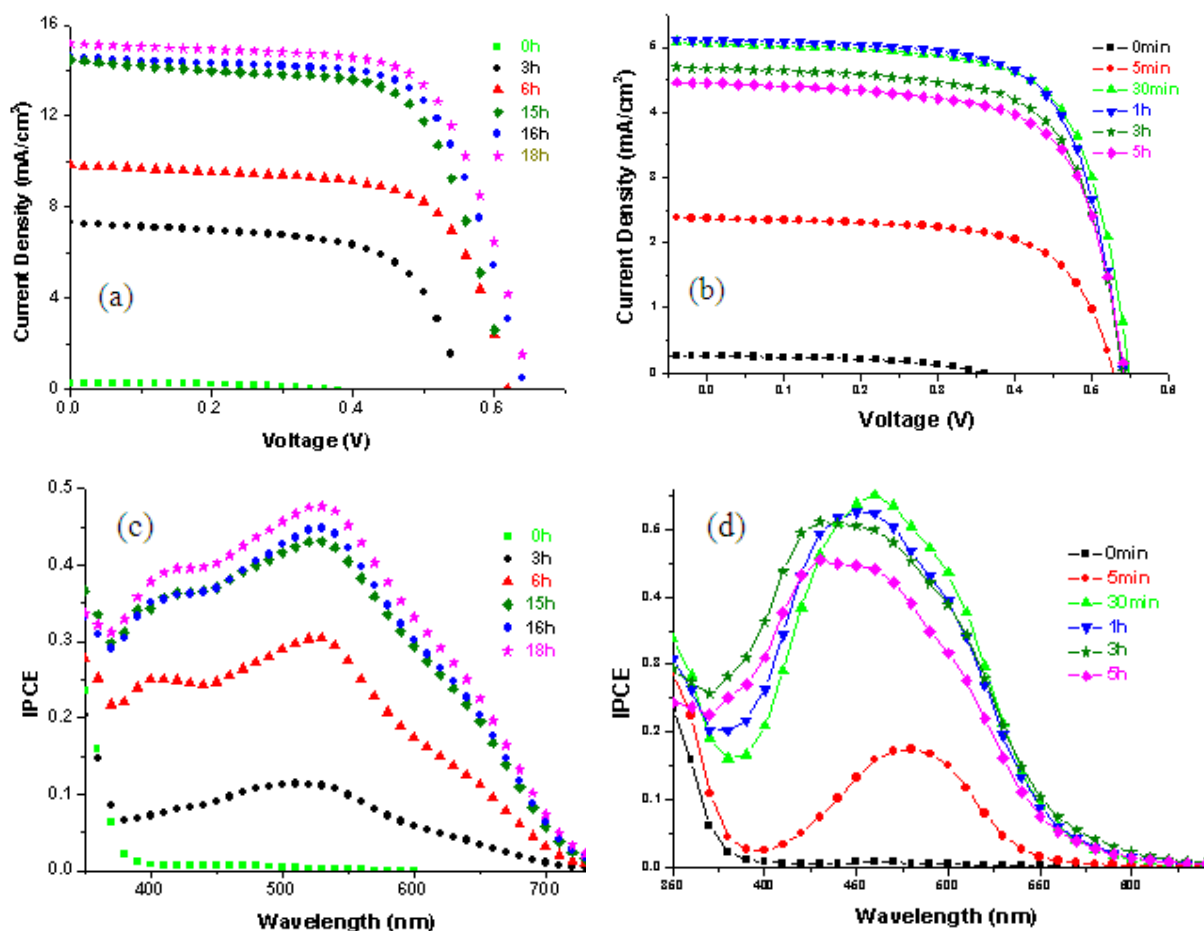


**Figure 7:** Current density-voltage curves for cells based on (a) Set 1(N719 adsorbed on  $\text{TiO}_2$ ) and (b) Set 2 (CT1 adsorbed on  $\text{TiO}_2$ ). IPCE curves of DSSCs based on (c) Set 1 and (d) Set 2, for different impregnation times.



In figure 8 the absorbance and the electrical results are compared. Panels (a) and (b) compare the cell efficiency and the absorbed number of moles as a function of impregnation time for Set 1 (N719/TiO<sub>2</sub> photoanodes) and Set 2 (CT1/TiO<sub>2</sub> photoanodes). In case of N719, the efficiency of the cell is increasing with increasing number of absorbed moles till the saturation point is reached. On the other hand efficiency of the cell based on hemisquaraine has been observed increasing up to 30min and then started decreasing regardless of increasing number of absorbed moles. This indicates that, for impregnation times higher than 1h, only a part of the hemisquaraine molecules present in the photoanode contribute to electric current generation. A consistent fraction of dye molecules is not able to transfer the photogenerated electron to TiO<sub>2</sub>, because they tend to aggregate each other or because their anchorage to TiO<sub>2</sub> surface is not effective. Moreover the non monotonic behavior of absorption spectra of the CT1/TiO<sub>2</sub> photoanodes (inset of figure 5b) evidence changes in the CT1 attachment to TiO<sub>2</sub>, in particular the peak at 565nm, appearing only after 1h, can be related to dye molecules aggregation.

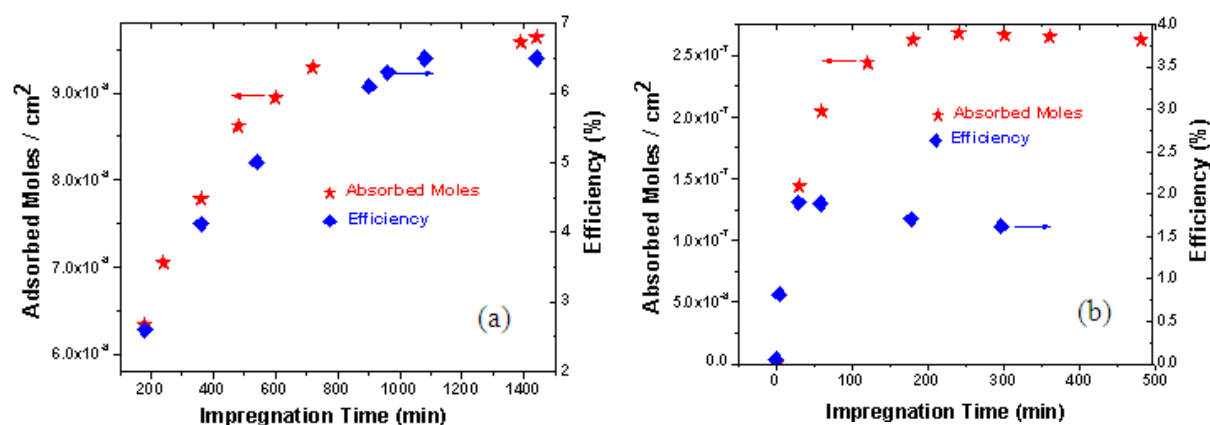


**Figure 8:** Number of absorbed moles has been compared with the efficiency of DSSCs based on:  
(a) Set 1, (b) Set 2.

#### 4.2. Sponge-like ZnO: absorption and electrical measurements

We performed impregnation time experiments also on ZnO-based photoanodes. A simple and low cost two-step method, based on RF magnetron sputtering deposition and thermal oxidation, for obtaining sponge-like ZnO nanostructured films has been recently proposed. These films exhibited a high density of branches, and a specific surface area of 14.1 m<sup>2</sup>/g. A photoconversion efficiency value of 6.67% was obtained with an 18  $\mu$ m thick film incubated with N719 dye molecules [15]. In this work 5  $\mu$ m thick sponge-like ZnO films were immersed in 0.25mM ethanolic solution of N719 dye (Set 3) and characterized for optical absorption (figure 9a). The results depict the strong absorption properties of ZnO films, up to 24 hours of incubation. The typical N719 peak (located at 530 nm) monotonically amplifies with increasing immersion time from 10 min to 5 hours. Only one very long (24h) impregnation time was measured and in the resultant absorption spectrum a radical change is observed: two new shoulder-like peaks appear at about 405nm and 480nm, and hence the peak at 530 nm is strongly broadened. This suggests an alteration in the N719 anchorage to ZnO surface for longer impregnation times. This hypothesis is also confirmed by the electrical characterizations (current density-voltage and IPCE curves) of DSSCs fabricated with these N719/ZnO photoanodes, given in figure 9 (b and c respectively). The best result is obtained for 2 hours of impregnation: it exhibits a short circuit current density ( $J_{sc}$ ) of 9.6 mA/cm<sup>2</sup> and an open circuit voltage ( $V_{oc}$ ) of 592 mV, leading to a maximum Photo Conversion Efficiency (PCE) value of 3.21%.

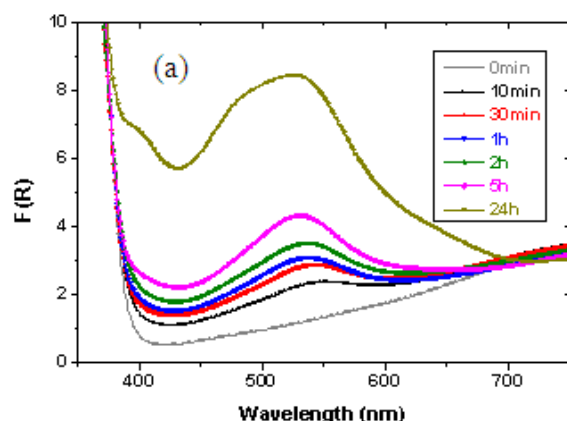
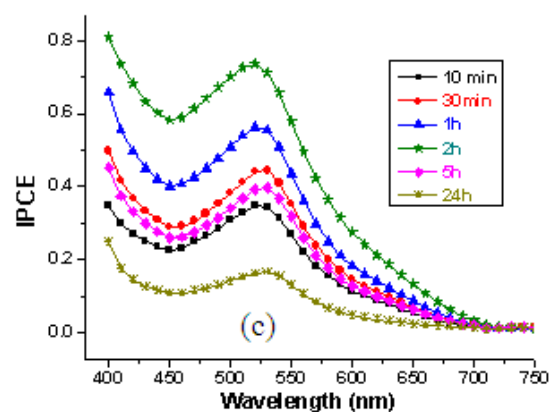
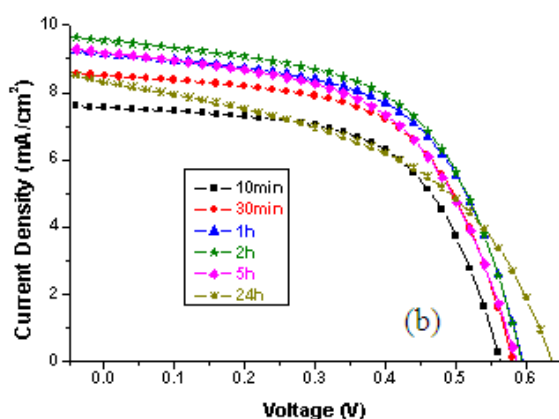


**Figure 9:** (a) Absorption spectrum of Set 3 (N719 dye absorbed on ZnO films), (b) Current density-voltage curve and (c) IPCE curves of Set 3 (solar cells based on sponge-like ZnO anode immersed in N719 solution) for different impregnation times.



The quantitative analysis results, obtained from depletion solution experiment, are reported in the inset of figure 10a. The number of absorbed dye molecules reaches a maximum at 1h and 45min, then it decreases and finally starts again to increase, with a different slope, at 2h and 20min. This indicates that nearly at 2h of impregnation the ZnO film stopped absorbing, and it released a few molecules to the solution, then it started absorbing molecules anew. The integrated dye absorbance reported in figure 10a, evaluated from  $F(R)$  results, confirms such increase in dye absorption up to 24h. In figure 10a the DSSC efficiency values are also reported: the most favorable incubation time results to be 2h: exceeding this time a decrease in efficiency is observed despite the increasing amount of dye loading, which is evident from both integrated dye absorbance and absorbed dye molecules. This can be related to the formation of molecular aggregates between dye molecules and dissolved  $Zn^{2+}$  ions instigating from the ZnO surface, as reported by several researchers [27, 28]. This dissolution of Zn surface atoms is caused by the acidic carboxylic groups of the N719 dye [13]. Drastic change in absorbance behavior after 24 hours of incubation also suggests the possible formation of new aggregates. Such molecular complexes show strong adsorption properties but are clearly unable to inject electrons in the conduction band of the semiconductor [19, 29].

Finally, some sponge-like ZnO substrates were also immersed in CT1 hemisquaraine dye solution (Set 4) and dye sensitized solar cells were fabricated using microfluidic approach to investigate their photon to electron conversion efficiency. As shown in figure 10b, this set remained unable to achieve efficiency higher than 0.65%. Such a low efficiency range was not enough encouraging for further investigations. The results obtained for all the different combinations of semiconducting oxide and dye are summarized in table 2.

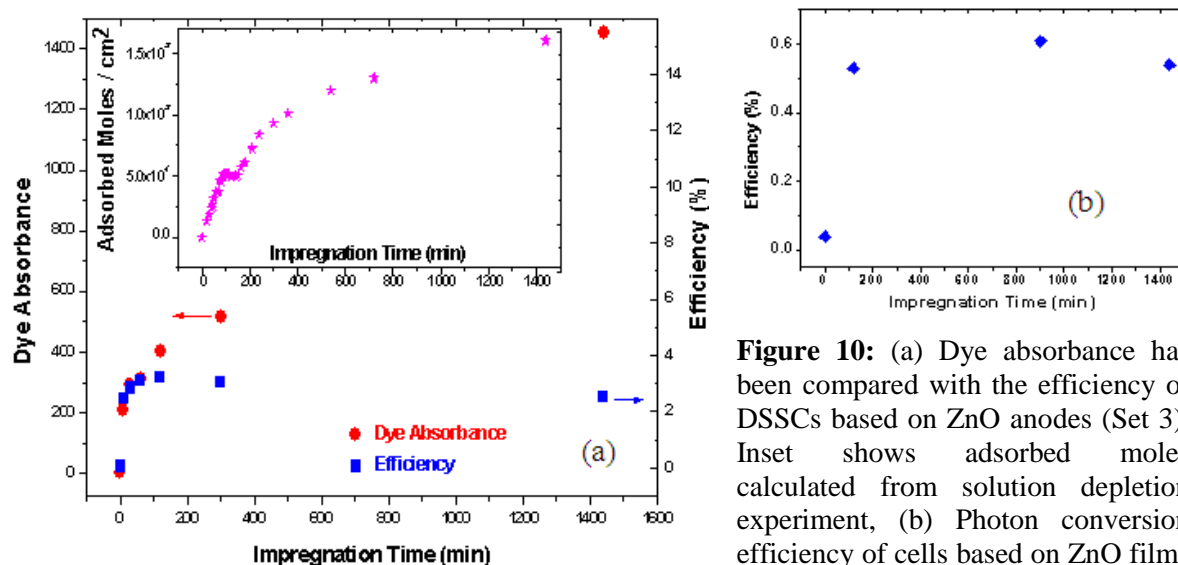


**Figure 10:** (a) Dye absorbance has been compared with the efficiency of DSSCs based on ZnO anodes (Set 3). Inset shows adsorbed moles calculated from solution depletion experiment, (b) Photon conversion efficiency of cells based on ZnO films immersed in hemisquaraine dye solution (Set 4).

**Table 2:** Summarized results.

	Favorable Impregnation time (hours)	Maximum Efficiency (%)	Absorption Behavior	Adsorbed Moles at Favorable time	Max Adsorbed Moles
Set 1	16	6.5	monotonic	$9.51 \times 10^{-8}$	$9.63 \times 10^{-8}$
Set 2	1	1.9	Non-monotonic	$14.5 \times 10^{-8}$	$25.5 \times 10^{-8}$
Set 3	2	3.2	Non-monotonic	$5.15 \times 10^{-8}$	$16.0 \times 10^{-8}$
Set 4	---	0.6	---	---	---

## 5. Conclusions

- We have employed three different UV-Vis absorbance measurements for monitoring the dye impregnation time of nanostructured photoanodes for dye sensitized solar cells.
- Two different dyes, the largely used Ru-based N719 and a recently proposed organic dye based on the hemisquaraine molecule, CT1, have been tested on two different semiconductor oxides: the traditionally employed nanostructured TiO<sub>2</sub> and a sponge-like ZnO film fabricated in our laboratory.
- Four different sets of dye impregnated semiconducting films have been used for dye sensitized solar cells fabrication, employing a microfluidic architecture; the cells have been electrically characterized by I-V and IPCE measurements.
- It has been shown that the analysis of the dye loading amount in photoanodes is helpful for interpretation of the conversion efficiency trend versus impregnation time, in view of optimization of the dying procedure.

## References:

- [1] O'Regan B and Grätzel M 1991 *Nature* **353** 737-740
- [2] Nazeeruddin M K, Kay A, Rodicio I, Humphry-Baker R, Mueller E, Liska P, Vlachopoulos N and Graetzel M 1993 *J. Am. Chem. Soc.* **115** 6382-6390
- [3] Nazeeruddin M K, Klein C, Liska P and Gratzel M 2005 *Coord. Chem. Rev.* **249** 1460-1467

- [4] Waston T, Holliman P and Worsley D 2011 *J. Mater. Chem.* **21** 4321-4325
- [5] Concina I, Frison E, Braga A, Silvestrini S, Maggini M, Sberveglieri G, Vomiero A and Carofiglio T 2011 *Chem. Commun.* **47** 11656-11658
- [6] Gratzel M 2009 *Accounts of Chem. Res.* **42** 1788
- [7] Jang S R, Yum J H, Klein C, Kim K J, Wagner P, Officer D, Gratzel M and Nazeeruddin M K 2009 *J. Phys. Chem. C* **113** 1998-2003
- [8] Gao F, Wang Y, Shi D, Zhang J, Wang M, Jing X, Humphry-Baker R, Wang P, Zakeeruddin S M, and Gratzel M 2008 *J. Am. Chem. Soc.* **130** 10720-10728
- [9] Choi H, Raabe I, Kim D, Teocoli F, Kim C, Song K, Yum J H, Ko J, Nazeeruddin M K and Gratzel 2010 *M Chem. Eur. J.* **16** 1193-1201
- [10] Cai N, Moon S J, Cevey-Ha L, Moehl T, Humphry-Baker R, Wang P, Zakeeruddin S M and Gratzel M 2011 *Nano Lett.* **11** 1452-1456
- [11] Im H, Kim S, Park C, Jang S H, Kim C J, Kim K, Park N G and Kim C 2010 *Chem. Commun.* **46** 1335-1337
- [12] Zhang Q, Dandeneau C S, Zhou X, and Cao G 2009 *Adv. Mater.* **21** 4087-4108
- [13] Ambade S B, Mane R S, Ghule A V, Takwale M G, Abhyankar A, Chod B W and Han S H 2009 *Scripta Mater.* **61** 12-15
- [14] Saito M and Fujihara S 2008 *Energy Environ. Sci.* **1** 280-283
- [15] Sacco A, Lamberti A, Gazia R, Bianco S, Manfredi D, Shahzad N, Cappelluti F, Ma S and Tresso E 2012 High efficiency Dye-sensitized Solar Cell exploiting sponge-like ZnO nanostructures. *Phys. Chem. Chem. Phys.* In Press, DOI: 10.1039/C2CP42705B
- [16] Cicero G *et. al.* 2012 Combined experimental and theoretical investigation of the hemisquaraine/TiO<sub>2</sub> interface in a dye sensitized solar cell. *Energy & Environmental Science* (submitted)
- [17] Demopoulos G P, Charbonneau C, Lee K E, Shan G B, Gomez M A and Gauvin R 2009 *ECS Trans.* **21** 23-34
- [18] Manmeeta, Saxena D, Sharma G D and Roy M S 2012 *Research Journal of Chemical Sciences* **2** 61-71
- [19] Lamberti A, Gazia R, Sacco A, Bianco S, Quaglio M, Chiodoni A, Tresso E and Pirri C F 2012 Coral-shaped ZnO nanostructures for dye-sensitized solar cell photoanodes *Prog. Photovolt: Res. Appl.* In Press, DOI: 10.1002/pip.2251
- [20] Lamberti A, Sacco A, Bianco S, Giuri E, Quaglio M, Chiodoni A and Tresso E 2011 *Microelectron. Eng.* **88** 2308-2310
- [21] Katoh R, Yaguchi K and Furube A 2011 *Chem. Phys. Lett.* **511** 336-339
- [22] Hwang K J, Yoo S J, Jung S H, Park D W, Kim S I, and Lee J W 2009 *Bull. Korean Chem. Soc.* **30** 172-176
- [23] Stergiopoulos T, Ghicov A, Likodimos V, Tsoukleris D S, Kunze J, Schmuki P and Falaras P 2008 *Nanotechnology* **19** 235602-235609
- [24] Koo H J, Kim Y J, Lee Y H, Lee W I, Kim K, and Park N G 2008 *Adv. Mater.* **20** 195-199
- [25] Yum J H, Walter P, Huber S, Rentsch D, Geiger T, Nüesch F, Angelis F D, Grätzel M, and Nazeeruddin M K 2007 *J. Am. Chem. Soc.* **129** 10320-10321
- [26] Andersen A R, Halme J, Lund T, Asghar M I, Nguyen P T, Miettunen K, Kemppainen E and Albrektsen O 2011 *J. Phys. Chem. C* **115** 15598-15606
- [27] Keis K, Lindgren J, Lindquist S E and Hagfeldt A 2000 *Langmuir* **16** 4688-4694
- [28] Memarian N, Concina I, Braga A, Rozati S M, Vomiero A and Sberveglieri G 2011 *Angew. Chem. Int. Ed.* **50** 12111-12366
- [29] Zhang Q, Chou T P, Russo B, Jenekhe S A and Cao G 2008 *Angew. Chem. Int. Ed.* **47** 2402-2406